

Formation of the vulva in *Caenorhabditis elegans*: a paradigm for organogenesis

Ranjana Sharma-Kishore¹, John G. White^{2,*}, Eileen Southgate² and Benjamin Podbilewicz^{1,2,‡}

¹Department of Biology, Technion-Israel Institute of Technology, Haifa, 32000, Israel

²MRC Laboratory of Molecular Biology, Hills Road, Cambridge, UK

*Present address: Laboratory of Molecular Biology and Department of Anatomy, University of Wisconsin, Madison, WI 53704, USA

‡Author for correspondence (e-mail: podbilew@tx.technion.ac.il)

Accepted 25 November 1998; published on WWW 20 January 1999

SUMMARY

The genes involved in the inductive interactions that specify cell fates in the vulva of *Caenorhabditis elegans* are known in some detail. However, little is known about the morphogenesis of this organ. Using a combination of cell biological and anatomical approaches, we have determined a complete morphogenetic pathway of cellular events that lead to the formation of the vulva. These events include reproducible cell divisions, migrations, remodeling of adherens junctions, cell fusions and muscle attachments. In the course of these events, an epithelial channel comprising

a stack of 7 toroidal cells is formed that connects the internal epithelium of the uterus with the external body epithelium, forming the vulva. Vulval muscles attach to the epithelial channel and the whole structure everts during the final molt. The mature vulva has rotational, two-fold symmetry. Using laser microsurgery, we found that the two halves of the vulva develop autonomously.

Key words: Morphogenesis, Vulva, *Caenorhabditis elegans*, Cell fusion, Cell migration, Adherens junctions, Cell fate

INTRODUCTION

Morphogenesis is one of the most striking manifestations of the development of a multicellular organism, but one that is as yet poorly understood. Organismal morphogenesis is often modular, producing discrete, non-overlapping organs such as the eye or kidney. Focused studies of organogenesis allow knowledge of development to be acquired piecemeal. In vertebrates, the development of organs such as the kidney (Saxen and Sariola, 1987), bone (Reddi, 1994), tooth (Thesleff and Nieminen, 1996) and placenta (Cross et al., 1994) have been subjected to considerable scrutiny. These studies have revealed insights into the process of tissue patterning and are beginning to provide information about mechanisms that specify cell identity. Developmental genetic studies of organisms such as *Drosophila melanogaster* or *Caenorhabditis elegans* have revealed signal transduction pathways that specify cell identity (Freeman, 1997; Kornfeld, 1997). In particular, studies directed towards the development of the eye in *Drosophila* (Banerjee and Zipursky, 1990) and the vulva in *C. elegans* (Horvitz and Sternberg, 1991) have revealed the inductive interactions and the signaling pathways that are used to generate the diversity of component cells that go to make up these organs (Greenwald and Rubin, 1992). Organogenesis in animals involves the remodeling of epithelia into organs (Trinkaus, 1984). In this study, we have determined the precise remodeling of 22 epithelial cells into an organ. We have endeavored to complement the considerable genetic studies

that have been made on the *C. elegans* vulva by determining the cellular basis of organogenesis of the vulva.

Background

Vulval development involves very few cells, occurs over a period of 20 hours, can be observed in living animals and can be analyzed by genetic and molecular methods. During the first larval stage, a linear sequence of 12 ventral hypodermal cells P(1-12).p is generated. In wild-type hermaphrodites, P(1-2).p and P(9-11).p fuse with the surrounding syncytial hypodermal cell (hyp7) (Sulston and Horvitz, 1977). Six vulval precursor cells (VPCs; P(3-8).p) are competent to generate vulval cells (Sulston and White, 1980). A somatic gonadal cell, the anchor cell (AC), induces the nearby P5.p, P6.p and P7.p to adopt vulval cell fates (Kimble, 1981) and the remaining three VPCs usually divide once and fuse with hyp7 (3° sublineage) (Kimble, 1981; Sulston and White, 1980). VPCs induced to adopt a vulval fate signal laterally to each other causing P5.p and P7.p to adopt a 2° sublineage and P6.p to adopt a 1° sublineage (Greenwald, 1997; Sternberg and Horvitz, 1989). Each sublineage (1°, 2° and 3°) consists of a distinct pattern of cell divisions generating a characteristic number and types of cells. Without the inductive signal from the AC, all VPCs fuse to hyp7 and no vulva is formed (Kimble, 1981; Sulston and White, 1980). There might be an independent signal from hyp7 dependent on the products of *lin-15* locus that represses a vulval fate or promotes a hyp7 3° (fused) fate (Herman and Hedgecock, 1990). The 2° sublineages require the product of

lin-12 gene in order to occur while the 1° sublineage is independent of *lin-12* activity (Greenwald et al., 1983).

Classic and molecular genetic analyses have shown that the inductive signal from the anchor cell is a molecule similar to mammalian growth factors encoded by the gene *lin-3*. A receptor tyrosine kinase (LET-23) on the surface of the VPCs is proposed to bind LIN-3 and activate a signal transduction cascade involving LET-60 Ras and MPK-1/SUR-1 MAP kinase. MAPK and its targets in *C. elegans* appear to be required for the decision between vulval and epidermal fates (for review, see (Greenwald, 1997). Epidermal fates in nematodes involve cell fusion as an important developmental decision during the morphogenesis of many organs (Baird et al., 1991; Podbilewicz and White, 1994; Sommer, 1997; Wang et al., 1993).

MATERIALS AND METHODS

Nematode strains, growth in liquid culture and synchronization of populations

Wild-type (N2) *C. elegans* was cultured as described (Brenner, 1974). A one-liter liquid culture of nematodes was grown and collected by sucrose flotation. Eggs were obtained by digesting this population with a final concentration of 1-2% alkaline hypochlorite and allowed to hatch overnight in liquid medium without food. The L1s so generated were collected by centrifugation, washed in M9 and allowed to grow in liquid medium with food. Aliquots were collected at 2 hour intervals (from L3 to the adult stage) and the specific populations were collected by sucrose flotation (Sulston and Hodgkin, 1988).

Permeabilization and fixation of worms

The different worm aliquots were resuspended in fixation buffer (Finney and Ruvkun, 1990) and 20% para-formaldehyde (Sigma) was added to a final concentration of 1%. All permeabilization, fixation and subsequent antibody-staining reactions were performed in 1 ml Eppendorf tubes (Finney and Ruvkun, 1990). A fraction of the worms were fixed using methanol-acetone, with the same results (Podbilewicz, 1996; Podbilewicz and White, 1994).

Immunofluorescence and confocal microscopy

Aliquots of the different fixed worm populations were washed with PBS-BSA (0.1%)-Triton X-100 (0.5%). Cell adherens junctions were visualized by staining with the monoclonal antibody MH27 (Francis and Waterston, 1991) and nuclei were stained with propidium iodide (Podbilewicz, 1996; Podbilewicz and White, 1994). The specimens were analyzed using a MRC-1024, laser confocal scanning microscope (Bio-Rad, Hemphstead, UK) with the objective Nikon Plan Apo 60×/1.40. Projections were obtained from 10-20 serial optical sections collected every 0.5 μm, in the z-axis. Figures are oriented with the anterior of the worm on the left-hand side of the page and are ventral views unless specified. Developmental timings were estimated from the size of animal and from studying the developing vulva with Nomarski optics using a Nikon Eclipse E-800 microscope. For all descriptions, at least 20 animals were observed and all developed as described, except where noted. Cell lineages were followed using Nomarski optics (Sulston and Horvitz, 1977). Serial EM reconstructions and laser microsurgery were performed as described (Sulston and White, 1980; White et al., 1986).

RESULTS

Formation of the vulva

Morphogenesis of the vulva in the wild-type hermaphrodite

The process of vulva formation can conveniently be split into

three phases. In the first phase (**execution and short-range migrations**), 22 epithelial cells are produced and migrate relative to their neighbors to take up their final configuration and form a tube containing 7 rings (toroidal cells) that join the endothelium of the uterus to the external epithelium (Fig. 1). The second phase is characterized by **cell fusions** within the 7 rings, vulval muscle attachments at defined regions and specific vulval cell attachments to lateral epithelial cells. The second phase covers most of the L4 stage. In the third phase (**eversion**), the vulva partially everts (turns inside out) at the L4 to adult molt and the lumen closes to block the transit of eggs until it is opened by activation of the vulval muscles.

To study developing organs, we obtained 3-dimensional reconstructions of confocal optical sections of vulvae stained with an antibody that recognizes the adherens junctions (apical surfaces and boundaries between cells) together with serial section electron microscopy. This approach reveals the construction of the organ involving short-range cell migrations and cell fusions (Podbilewicz and White, 1994).

First phase of vulva formation (execution and short-range migrations)

To study cell migrations, cell fusions and formation of cell junctions with the hypodermis, we reconstructed intermediates in the early stages of vulva morphogenesis. The first phase covers the division of the vulval precursor cells (VPCs) to the termination of the vulval lineages at the end of the L3 stage (Figs 2, 3).

P3.p, P4.p and P8.p are ventral epithelial cells that have the potential to generate vulval cells (Sulston and White, 1980) but in wild-type animals they divide and fuse with hyp7, the larger hypodermal syncytial cell that surrounds the VPCs. Induced P5.p, P6.p and P7.p undergo two rounds of division and form a linear row of 12 epithelial cells situated on the ventral midline (Fig. 1). EM and confocal reconstructed vulval primordia after the first and second rounds of VPC division exhibited no signs of differentiation. Fig. 2 shows confocal reconstructions of the apical domains of vulval precursors stained with the MH27 monoclonal antibody (Francis and Waterston, 1991) that binds at, or close to, adherens junctions during (Fig. 2A) and after (Fig. 2B,C) the second round of longitudinal division. In summary, during the first two divisions all cells divide longitudinally and there is an apparent bilateral symmetry; however, there is some degree of asymmetry between the anterior and posterior halves of the vulvae (e.g. Fig. 2B). During the terminal (third) round of divisions, six cells divide transversely, two cells do not divide and four divide longitudinally (Fig. 1). Fig. 2 shows examples of VPC granddaughters during the third round of division. The precursors of **vulE** (P6.ppp and P6.paa) are the first to divide transversely (Fig. 2D) and in general the anterior half of the vulvae develops faster than the posterior half (Fig. 2E).

One EM reconstruction of a vulval primordium at the intermediate stage (not shown) in which the first terminal divisions of the VPCs had just occurred shows four daughter cells that migrate towards the center of symmetry of the vulva (where the anchor cell is situated). The four cells form a square configuration (precursor to **vulE**) with a hole in the middle displacing the central two cells dorsally (**vulF**). Few signs of morphogenesis were detected in the other vulval cells in this EM reconstruction and in similar intermediates reconstructed with the confocal microscope (Fig. 2F). Fig. 3 shows ventral views

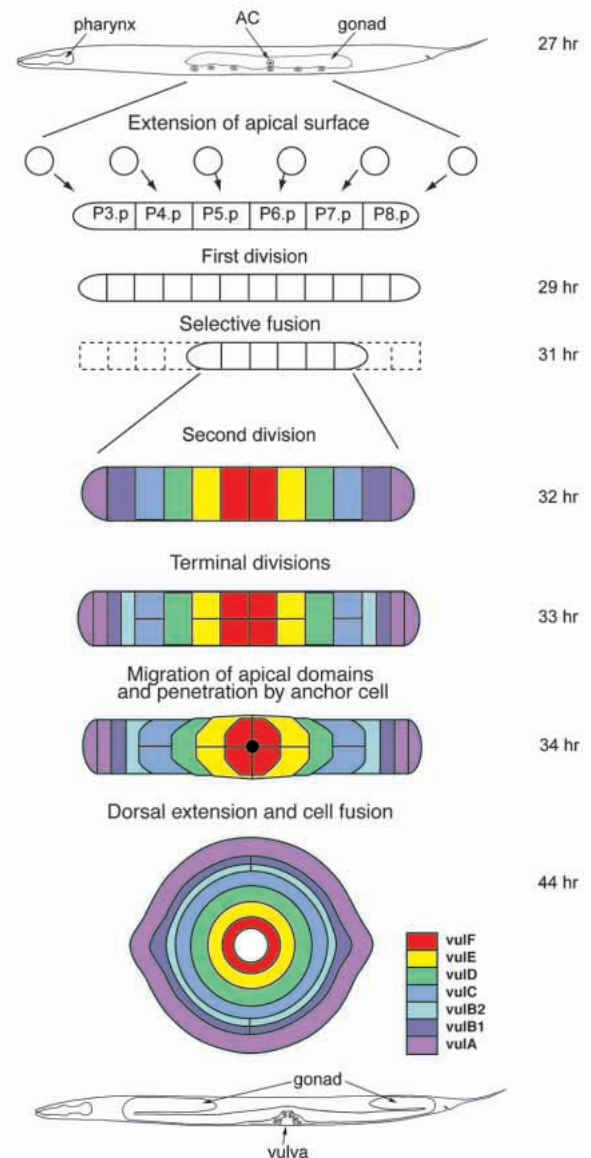
of intermediates in different stages of early morphogenesis and ring formation. Fig. 3B shows an intermediate vulva reconstructed with the confocal microscope that has a central ring precursor containing four cells (**vulF**), four cells that surrounded the central ring form the next ring (**vulE**) and a third ring with two cells (**vulD**). The next two cells on each side (**vulC** precursors) have divided transversely and are sending processes towards the center of symmetry of the vulva surrounding **vulD**. The outer cells on each side are the precursors of **vulA** that fused (see Fig. 3A before cell fusions) and will be the last to migrate. A second EM reconstruction of a vulva just after the terminal round of divisions revealed intermediate stages of the short-range migrations (Fig. 4A,B ventral and lateral views respectively). The cells that will form **vulC** and **vulD** had sent processes that displaced the adherens junctions that were between the central vulval cells (the precursors of rings **vulE** and **vulF**) and the hypodermal cell (**hyp7**). Precursors to the more distal vulval rings (**vulA**, **vulB1** and **vulB2**) were further behind developmentally with **vulB2** sending out only a small extension and **vulA** showing no morphological changes (see also Fig. 3B). The innermost cells (the daughters of P6.pap and P6.ppa), making up the **vulF** ring formed a rectangle with the anchor cell nestling into a pocket in the middle (Fig. 4B). At slightly later times, the anchor cell breaks completely through the center of the group of four cells in the middle of the primordium thus forming the **vulF** ring. This second EM reconstruction and confocal reconstructions (e.g. Fig. 3) revealed how the series of stacked epithelial rings that make up the vulva is formed out of a row of 22 epithelial cells. These observations show that short-range cell migrations in the vulva primordium involve rearrangements of adherens junctions, as shown for other

migrations in *C. elegans* (Podbilewicz and White, 1994), sea urchin (Hardin, 1989), *Drosophila* (Grawe et al., 1996) and other organisms (Yap et al., 1997).

In a temporal sequence, starting in the center i.e. proximal to the anchor cell, vulval primordial cells (VPC grand and great-granddaughters; Fig. 1) send out unidirectional extensions towards the center of the primordium that displace the adherens junction between **hyp7** and the inner, neighboring precursor cell. This process begins with the **vulE** cells, each of which sends out two lateral extensions towards the vulval midline. Towards the center of the primordium, these extensions become stacked up, with the processes from the outer cells running ventral to those of their inner neighbors. These process-like extensions interdigitate between the two displaced cells, forming their own adherens junctions giving rise to a 'Y' configuration of junctions at the apex (Figs 3, 4). This structure is situated right out at the tip of the extending process suggesting that the act of opening up and reforming the junctions may be part of the driving force for process extension.

In summary, organogenesis begins with the final round of

Fig. 1. Schematic representation of the cellular events that occur during the morphogenesis of the vulva in *C. elegans*. The top diagram (lateral view) represents a larva in the L3 stage. A somatic gonadal cell, the anchor cell (AC), through inductive signaling induces three (P5.p, P6.p and P7.p) of the six vulval precursor cells (VPCs), P3.p to P8.p, to adopt vulval fates. The non-vulval cells- P3.p, P4.p and P8.p undergo a single proliferation step and fuse with the underlying syncytial cell. The remaining three VPCs signal laterally to each other to adopt fates that involve distinct patterns of cell divisions and generate specific numbers and types of cells. The cells of the vulva primordium perform short-range migrations from the outer regions towards the central midline, in a symmetrical fashion and also undergo fusions with specific partners. This involves the cells adjacent to the innermost cells forming processes and migrating around them (i.e., precursor cells of the ring **vulE** send processes around the precursor cells of the inner ring **vulF**). This process is repeated in a temporal sequence by the next outer cells that send processes around their inner neighbours, which meet at the midline. This results in the formation of a stack of 7 toroids (**vulA** to **vulF**) at the center. This is followed by fusion between the component cells of each ring, in a specific and temporal order. The resultant structure is an epithelial tube that connects the uterus of the worm to the outside. The anchor cell (black circle in the center) eventually penetrates the inner ring (**vulF**) and fuses with a uterine cell (open white circle at the center). Diagrams are ventral views, the anterior of the worm on the left-hand side of the page and represent the apical domains of cells unless specified. The same color code for the different cell types and the vulval rings has been maintained for all the figures. The vulva in the L4 stage (last diagram; lateral view) appears like an invagination from the ventral side of the worm. Times given are hours from hatching at 20°C (Sulston and Horvitz, 1977).



division when symmetrical groups of cells on either side of the four central cells (precursors of **vulF**; Fig. 3) send out processes between **hyp7** and their inner neighbors. The precursors of **vulE** (the daughters of P6.paa and P6.ppp; Fig. 5) migrate ventrally and laterally towards the midline of the vulva where they form a ring of 4 cells connected by adherens junctions. The next ring of epithelium is formed when precursors of **vulD** migrate surrounding the first ring. In a similar fashion, more concentric rings of epithelium are formed. The process is sequential from inner to outer groups until 7 rings have formed.

Second phase of vulva formation (cell fusions within the 7 rings)

The anchor cell invades the center containing 4 cells making a hole in the middle that results in the formation of a central ring (called **vulF**); this ring attaches to the uterus via adherens junctions to the **uv1** cells. The anchor cell then fuses (Fig. 4C) with the precursors of the **utse** syncytium of the gonad (Newman et al., 1996). Cell fusions occur among cells within the rings (Figs 6, 7). The order in which the cells within the rings fuse is **vulD**, **vulA**, **vulC**, **vulF** and **vulE**. **vulD** is a binucleate cell and the pair of cells within **vulB1** and **vulB2** remain unfused, the other rings are tetranucleate. These 7 concentric rings are stacked (Fig. 5). The ring **vulE** sends processes to the seam lateral epithelial cells, vulval muscles attach to specific sites and **vulA** makes junctions with the syncytial hypodermal cell **hyp7** (Figs 8, 9).

The confocal reconstructions in Figs 6 and 7 show intermediates containing 7 rings that have completed the migrations and are in different stages of the cell fusions within each concentric toroidal ring. For example, the most external vulval ring adjacent to the external epithelium (**vulA**) was formed by the migration of the most external cells in Fig. 3. These cells fuse in pairs before they migrate (Fig. 3B), their processes meet in the center and form two adherens junctions between them (Fig. 6A). In an intermediate step between Fig. 6B and C, the two junctions disappear because the two binucleate cells fuse at two points forming the syncytial ring **vulA**, a cell containing four nuclei.

The epithelial rings of the vulva are attached to each other by means of circular adherens junctions (Figs 6, 7). These junctions, in common with those described in other epithelia (Podbilewicz and White, 1994), demarcate the apical and basal domains of epithelial cells. The organization of these junctions was reconstructed from EMs of serial sections (Fig. 4C-E) and in the light microscope by immunofluorescent staining with the MH27 monoclonal antibody (Fig. 6). The apical domains of the toroids are situated on their inside surfaces and together make up the internal luminal surface of the vulva.

The toroid at the dorsal end of the stack (**vulF**) is attached to the uterus (Newman et al., 1996). Four small, extended epithelial cells (**uv1**) arranged in a rhomboid configuration attach to **vulF**. The four **uv1** cells in turn are attached to a large syncytial uterine cell (**utse**) that has nine nuclei. The bulk of this cell is situated on each side of the uterus and appears to be used to attach the uterus to the lateral epithelial cells (Fig. 8).

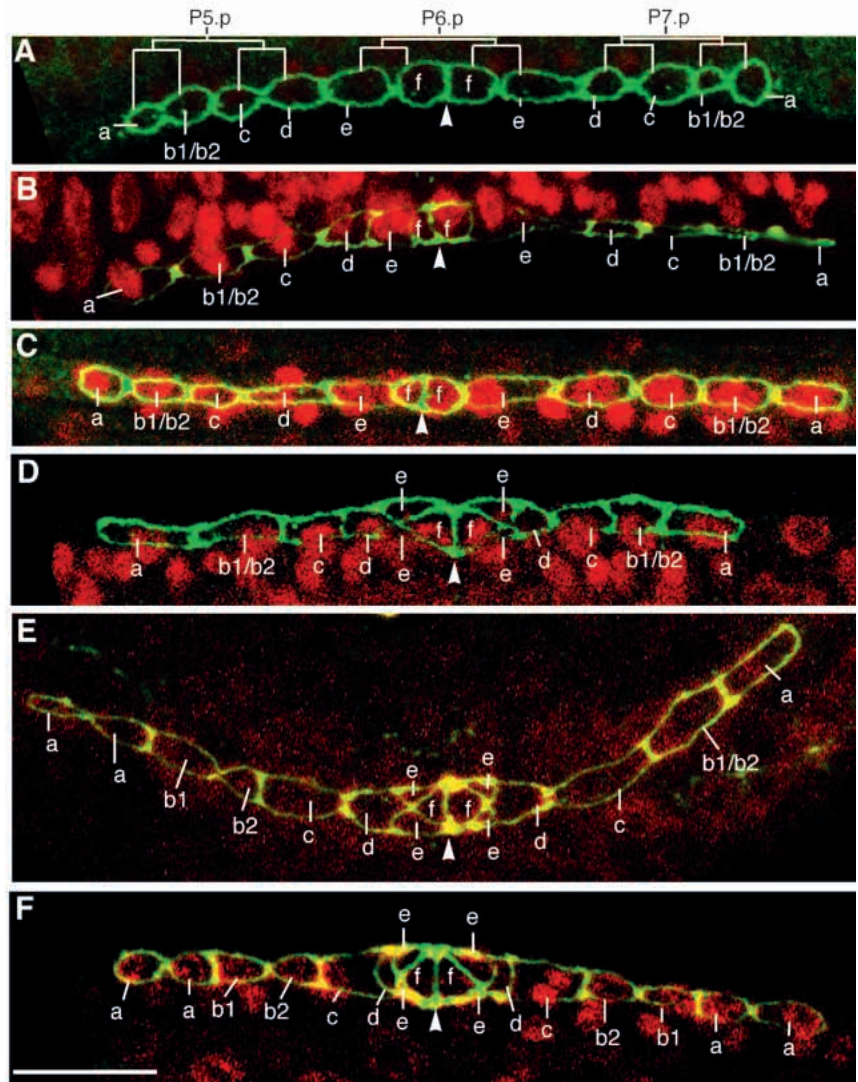


Fig. 2. Proliferation of vulval precursor cells. Confocal micrographs of early L3 vulvae stained with the nuclear stain propidium iodide (red) and MH27 mAb (green) that reveals apical domains of cells (Francis and Waterston, 1991; Podbilewicz, 1996; Podbilewicz and White, 1994). Pictures were obtained by projecting 5-10 serial confocal sections of 0.5 μm . All estimated times are in hours after hatching. (A) Ventral view of vulval primordium showing the 12 resultant grand-daughters of the VPCs, P5.p, P6.p and P7.p, after two rounds of cell division; grand-daughters of P5.p and P7.p are still undergoing cytokinesis; a, b1, b2, c, d, e and f are the precursor cells of the future vulval rings – **vulA** to **vulF**, respectively (approximately 31.5 hours). (B) Oblique view of an asymmetric vulva. The posterior precursor of E (P6.ppp) is twice as long as the anterior precursor of E (P6.paa). (C) Symmetric primordium with the 12 granddaughters of the VPCs. (D) Oblique view of 14 cell intermediate; precursors of **vulE** have divided, resulting in four E cells. (E) Ventral view of asymmetric primordium with precursors of **vulA** and **vulB**s having divided in the anterior half, resulting in the cells B1 and B2, and two A cells. (F) Ventral view of symmetrical 18 cell primordium where the terminal divisions of A, B1, B2 and E are completed (32.5 hours), before the terminal divisions of **vulC** and **vulF** precursors. Arrowhead, centre of symmetry. Scale bar, 10 μm .

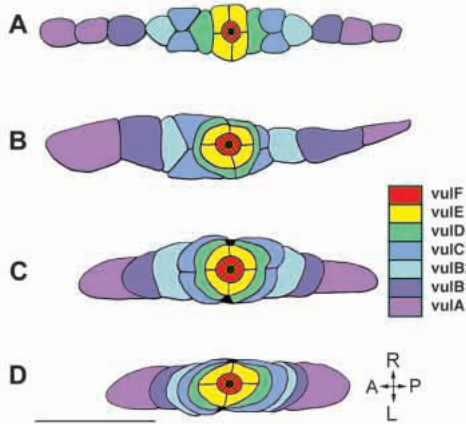


Fig. 3. Early morphogenesis of vulval cells. Apical domains of the cells are visualized by using the mAb MH27 that recognizes adherens junctions. Pictures were obtained by projecting 10-15 confocal serial sections of 0.5 μm . The schematic drawings are ventral views based on these pictures with the anterior of the worm on the left-hand side of the page. (A) Intermediate with all 22 vulval cells (34 hours); **vulC** precursors have divided, resulting in four C cells; the four **vulE** precursors surround and push **vulF** precursors dorsally. (B) Intermediate where **vulD** precursors have migrated to surround the inner ring precursors of **vulE** and **vulF** (35 hours); **vulC** precursors are sending processes from each side, around the inner **vulD** precursors; **vulA** precursors on each side have fused in pairs, in a longitudinal fusion (F_L). (C) Intermediate where the processes from **vulC** precursors on each side are being extended towards the central midline (36 hours); **vulB1**, **vulB2** and **vulA** precursors have started sending processes around their inner neighbors, towards the central midline. (D) Intermediate where **vulC** precursors have fused in pairs on each side, in a transverse fusion (F_T), and have sent processes towards the midline where they have met (37 hours); adherens junctions are seen at the point of contact, indicating that the fusions of the component cells for the **vulF**, **vulE**, **vulD** and **vulC** rings have not yet taken place. Closed black circle at the center represents the anchor cell that invades and penetrates the four **vulF** precursor cells. (A, anterior; P, posterior; R, right; L, left). Scale bar, 10 μm .

A thin sheet from the **utse** cell interposes between the **uv1** cells and the adjacent **uv2** cells to form a barrier separating the lumen of the vulva from the lumen of the uterus (Newman et al., 1996). This region of the **utse** cell apparently has two separated apical domains: one adjacent to the lumen of the uterus and one adjacent to the lumen of the vulva. This structure probably acts as a hymen and would be ruptured when eggs pass through the vulva. **vulE** has lateral extensions that attach to the lateral seam cells of the body in the same region as the **utse** cells of the uterus attach (Figs 8, 9B). These attachments probably prevent the vulva/uterus from prolapsing after the final molt. The **vulE** cell also seems specialized in that nerve processes from the VC and HSN motor neurons that innervate vulval muscles grow out along the lateral extensions of this cell (White et al., 1986). There are two sets of four vulval muscles, the **vm1** and the **vm2s** that link the vulva to the body wall. It seems likely that these attachment points are specific, as they are invariably located in the regions depicted in Fig. 8.

Third phase of vulva formation (from the L4 to the adult molt)

EM reconstructions and Nomarski observations in living late

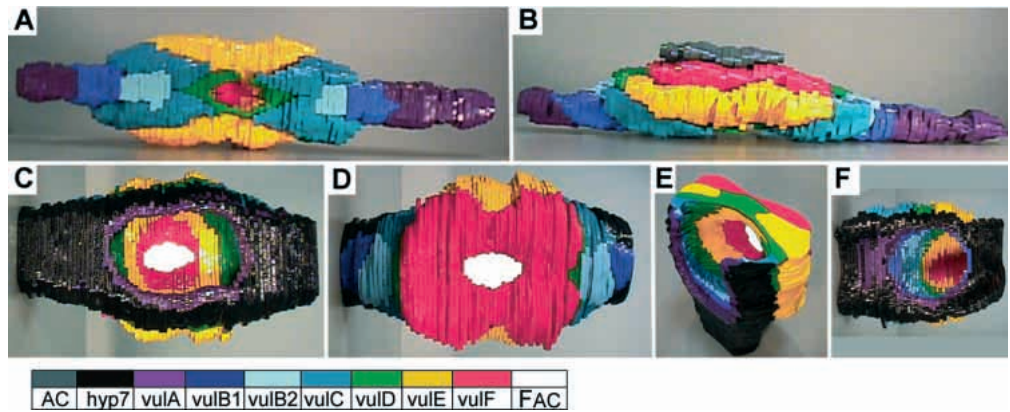
L4s and early adults show that cuticular material is secreted in a polarized way to the lumen of the vulva and the vulval labia are formed. Confocal reconstructions of everted vulvae show that **vulB1** and **vulB2** remain unfused ($n=5$; data not shown). After vulva eversion, the lumen closes preventing the transit of eggs until it is opened by the action of the vulval muscles. The structure of the adult vulva is accomplished without major relative cell movements. The final structure is reached by plastic deformations of the immature L4 vulva from the second phase.

In summary, the vulva in the fourth larval stage (L4) of *C. elegans* consists of a tube made of a stack of 7 toroidal cells with the anchor cell in the apex of this tube connecting to the uterus (Fig. 5). During the L4, the anchor cell fuses to the **utse** uterine multinucleated cell causing the opening of the tube (Figs 4C-E, 7). The vulva then everts to form a mature adult vulva through which eggs can be laid.

Laser microsurgery shows that each side of the vulva develops autonomously

The developing vulva has a mirror-symmetric structure. As we have described above, during vulval morphogenesis cells from each side of the center line send two extensions towards the mid-line until they meet their symmetrical partners on the other side, thereby forming the stack of rings. It appeared as if each cell could be attracted towards its symmetrical partner. However, we observed that 27% ($n=55$ vulvae from the first phase) of the vulvae analyzed had developing rings containing asymmetric divisions and migrations (e.g. Figs 2B,E, 3B). In general, the anterior half of the vulva developed faster suggesting that the two halves of each ring precursor develop autonomously. We tested this possibility by removing one half of the cells of a developing primordium with a laser microbeam. We killed the posterior three cells of a six-cell primordium (just after the first division of the VPCs). The half vulva appeared to develop normally except that the terminal division of the P6.pap cell (giving rise to the cells of the **vulF** ring) was longitudinal instead of transverse. To analyze the cell migrations and cell fusions within the semi-vulva, this animal was reconstructed from electron micrographs of serial sections. We found that the two components of the **vulF** cell looked normal in that the anchor cell was deeply embedded in them and they made adherens junctions to uterine cells. Thus, the cells seemed to have acquired the same differentiated state in spite of being daughters of a longitudinal division instead of the normal transverse division. In addition, all the cells had sent out two extensions in the normal way, to what would have been the mid-line of the vulva (Fig. 4F) However, instead of contacting their symmetrical partners, they had grown around the primordium until they contacted themselves (Fig. 9C). In several toroids, these processes had actually fused forming a complete ring (Fig. 9D). Therefore, we propose that, in the absence of a corresponding ring precursor partner on the opposite side, the two processes can continue migrating until they contact each other. This can prevent their further migration and eventually promotes 'self' fusion. In summary, the events that can occur in the absence of half the precursors are cell migrations, stacking of 7 rings, fusions within the rings and generation of a functional semivulva. Taken together, the resulting semivulva and the high incidence of asymmetric vulvae suggest a model in which at least two positive signals, one originating from the adjacent dorsally located ring and the other coming from the ventrally located hypodermal

Fig. 4. Three-dimensional models of EM serial sectioned vulvae. These are wooden models where each transverse section was cut and painted based on a tracing of an electron micrograph and assembled in the same order as the sections, to produce a scale model of the cells comprising the vulva. Vulval cells are color coded as in Fig. 1. (A) Ventral view of an early L4 vulva (similar developmental stage as in Fig. 3B) where **vulD** precursors have migrated to surround the inner ring precursors of **vulE** and **vulF**; **vulC** precursors are sending processes from each side, around the inner **vulD** precursors; **vulB2**, **vulB1** and **vulA** precursors on each side have not started the process of migration and toroid formation. (B) Left-lateral view of the same model as in panel A, showing the anchor cell (in gray) sitting on top of **vulF**; the newly formed rings **vulE** and **vulF** were pushed dorsally (up) by the ventral migration of the next ring (**vulD**). (C) Ventral view of a late L4 vulva where all the rings have formed and after the anchor cell has fused (**FAC**, fused AC is a hole in the middle in white). (D) Dorsal view of the same model shown in C. (E) Partial vulva, photographed after removing half of the model; this is an oblique transverse view of the same vulva from C and D showing the central hole, contours of the rings and a single transverse cross-section on the top with the boundaries of three rings. (F) ventral view of a semi-vulva, in which, we killed the posterior three cells of a six-cell primordium (just after the first division of the VPCs), in the absence of the posterior half, the anterior half has developed autonomously forming 7 rings (see Fig. 9 for more details). The sections painted in black in C-F represent the hypodermal cell **hyp7**. Figures are oriented with the anterior of the worm on the left, unless specified.



syncytium, attract the growing processes to open the junctions between them. The physical interaction between the opposing tips of the growing processes constitutes a third signal in our model for the arrest of further migration.

Summary of sequence of events in vulva formation

Our studies, along with previous genetic and cell ablation studies (reviewed in Greenwald, 1997), suggest that the following sequence of events occurs during the organogenesis of the vulva:

(1) An EGF-like signal (**LIN-3**) from the anchor cell defines three adjacent epithelia cells, **P5.p**, **P6.p** and **P7.p** (or their six daughters) as vulval precursors (possibly by inhibiting fusion). **P3.p**, **P4.p** and **P8.p**, which are more distal from the **AC**, divide once and their daughters fuse with the hypodermal syncytium **hyp7**.

(2) Lateral signaling among the vulval precursors using a **LIN-12** signal (and possibly other unidentified signals) establishes a set of six cell fates (**A**, **B**, **C**, **D**, **E** and **F**). The cell fates are established in a palindromic sequence along the single row of vulva precursor cells (Figs 1, 5).

(3) The terminal divisions of **C**, **E** and **F** are transverse, this being orthogonal to the previous divisions of the precursors. This event marks the start of vulva morphogenesis. The anchor cell is positioned in the center of the four ventral **vulF** cells and starts to open up a central pore marking the beginning of lumen formation (Figs 1, 5).

(4) In a proximal-distal sequence, cells produced by the vulval lineage migrate towards

the center of the vulva primordium wrapping themselves around their proximal neighbors until they meet their symmetrical homologues on the other side of the vulva. In so doing, the central apex of the vulval primordium moves inwards (i.e. dorsally) to make a conical structure (Fig. 5). We have shown

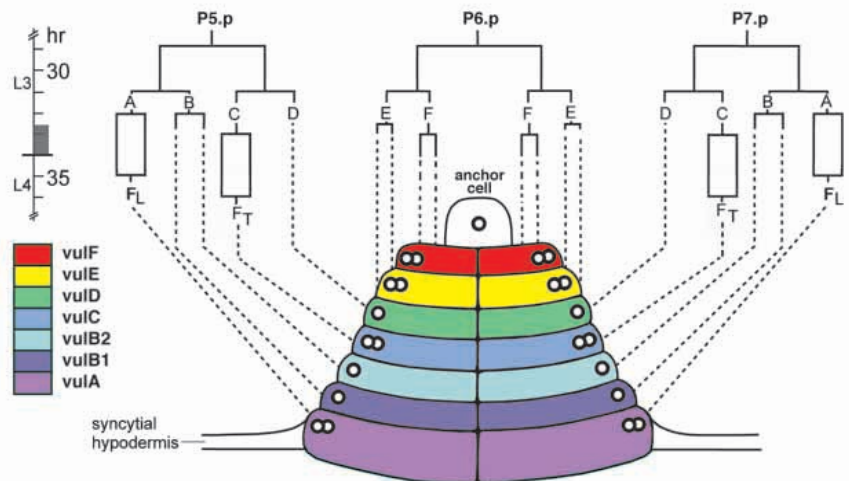


Fig. 5. Schematic representation of an early L4 vulva (~38 hours), showing the 7 rings stacked together, before the intratoroidal fusions, with the anchor cell at the top. The lineage relationships of the component cells of the rings are indicated with the divisions, fusions and migrations that the descendants of the VPCs – **P5.p**, **P6.p** and **P7.p**, undergo. Each VPC grandchild has unique properties. Thus, here we define a new nomenclature calling the VPC.xx cells **A**, **B**, **C**, **D**, **E** and **F**. In general **A** and **B** divide longitudinally (**L**), **C**, **E** and **F** divide transversally (**T**) and **D** does not divide (**N**). Vertical dotted lines begin in the lineage at the time that each cell begins to migrate and the diagonal portion of the dotted lines connects to the cell represented. The open rectangles represent a fusion before migration. Open circles represent nuclei. (**F_L**, longitudinal fusion; **F_T**, transverse fusion). All divisions are **L** (anterior-posterior) unless otherwise indicated. L3/L4 molt is indicated by a solid line on the time axis (hours after hatching), adjacent gray box indicates the period of lethargus, which occurs at each molt (Sulston and Horvitz, 1977).

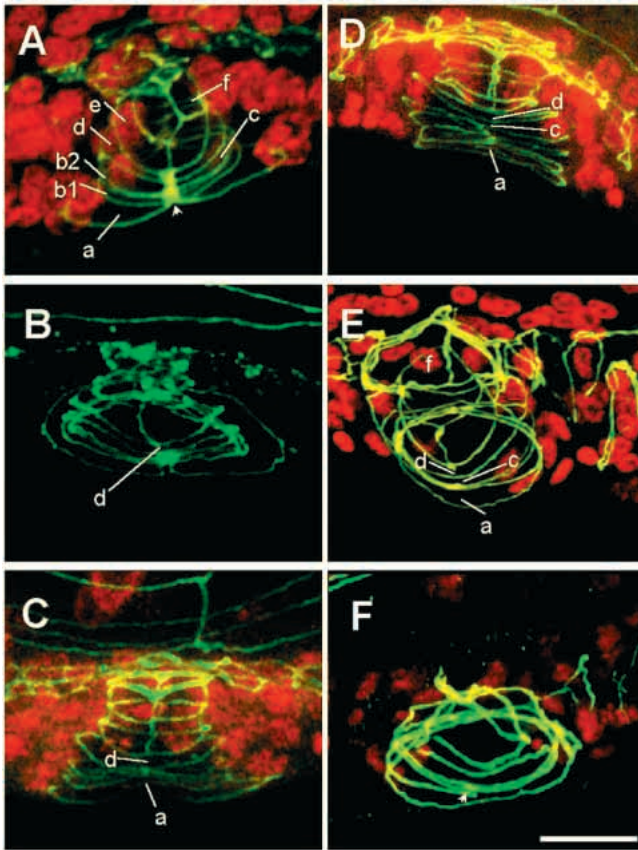


Fig. 6. Confocal micrographs of early and late L4 vulvae showing the apical domains of the 7 epithelial rings stained with MH27 mAb (green) and nuclei (red). Pictures were obtained by projecting 15–20 confocal serial sections of 0.5 μm . They represent the order in which the intratoroidal fusions occur (fusions within the rings occur). Presence of adherens junctions between the rings indicates absence of fusion within a ring. Disappearance of a junction between rings indicates an intra-ring fusion, specified with a line and labeled **a** to **f** (**vulA**–**vulF**). (A) Dorsolateral view of an intermediate where no intra-ring fusions have occurred (38 hours). Arrowhead here shows adherens junctions between the outer rings. (B) Dorsolateral view of an intermediate where only **vulD** has fused longitudinally. (C) Lateral view of an intermediate where **vulD** and **vulA** have fused. (D) Lateral view of an intermediate where **vulD**, **vulA** and **vulC** have fused. (E) Ventrolateral view of an intermediate where **vulD**, **vulA**, **vulC** and **vulF** rings have fused. (F) Vento-lateral view of an intermediate where **vulD**, **vulA**, **vulC**, **vulF** and **vulE** have fused (44 hours); arrowhead shows unfused adherens junctions in **vulB1** and **vulB2**. **VulF** at the top of the stack attaches to the uterus. **VulA**, **vulC** and **vulD** fuse longitudinally (F_{L}); **vulE** and **vulF** both fuse longitudinally and transversely. (F_{L} , intratoroidal longitudinal fusion; F_{T} , intratoroidal transverse fusion). Scale bar, 10 μm .

that this process occurs independently in each half of the vulva. Furthermore, EM studies of the multivulva mutant *lin-15(e1763)* have demonstrated that this process does not require the presence of the anchor cell (unpublished observations). It therefore seems as if a given cell in a sequence is programmed to wrap around its proximal neighbor in the sequence. This is the central process that transforms a linear array of epithelial cells into a hollow, conical vulva primordium.

(5) Concomitantly with the cell migrations described above,

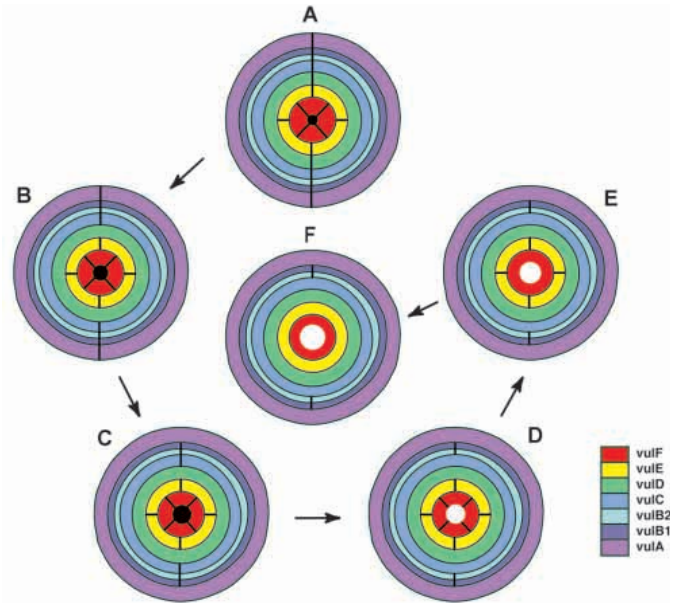


Fig. 7. Diagrammatic representation of the vulval rings showing the temporal sequence of the intra-toroidal fusions. The 7 concentric circles from the outside to the inside, in each diagram, represent the apical domains of rings **vulA** to **vulF**, respectively. Perpendicular lines within circles represent the junctions between component cells. Their disappearance indicates an intratoroidal fusion. Black circle at the centre represents the anchor cell, which invades and penetrates the four **vulF** precursor cells, and fuses with a uterine cell (white circle). The order of the intratoroidal fusions are **vulD** ($n=4$), **vulA** ($n=4$), **vulC** ($n=9$), **vulF** ($n=5$) and **vulE** ($n=2$), seen in B, C, D, E and F, respectively. (A) Representation of a vulva where all the rings are unfused ($n=21$). Rings are color-coded as in Fig. 1. Figures are oriented with the anterior of the worm on the left-hand side of the page and are ventral views.

a stereotyped sequence of homotypic cell fusions occurs transforming the vulva primordium into a sequence of toroidal syncytia (Figs 1, 7).

(6) The anchor cell undergoes a heterotypic cell fusion to a large uterine syncytium (**utse**) opening up the lumen of the vulva to the uterus (although a thin membrane of **utse** separates the vulval from the uterine lumens until the first eggs are laid). At this time, the attachment of the vulva primordium to the uterus becomes consolidated by means of the uterine **uv1** and **utse** cells.

(7) Vulval muscles attach to specific regions of the vulva and the **vulE** cell makes attachments to the lateral hypodermal (seam cells) (Fig. 8). The inner cuticular lining of the vulva and cuticle on the labia start to be secreted at this time. The morphogenesis of the vulva is now essentially complete.

(8) The last phase of development (eversion) occurs during the final molt and involves plastic deformations of the structure to form a valve that is opened by the contraction of the vulval and uterine muscles to allow eggs to be laid.

DISCUSSION

The cellular basis of pattern formation

We have defined a developmental pathway responsible for the formation of a simple organ. In summary, we have characterized all the cellular migrations and fusions required for the assembly

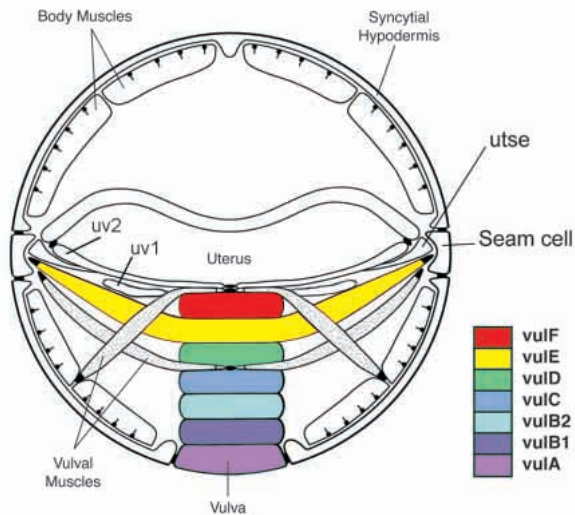


Fig. 8. Late L4 stage. Transverse section of the body in the region of the vulva and uterus shows various attachments. **VulF** makes adherens junctions with the **uv1** cells of the uterus, **vulE** attaches to the seam lateral epithelial cells and **vulA** makes junctions with the syncytial hypodermal cell, **hyp7**. There are two sets of four vulval muscles—**vm1s** and **vm2s**. **vm1s** are attached to the body wall at one end and to the vulva, between **vulC** and **vulD**, at the other. **vm2** muscles attach to the body wall more ventrally, and at their proximal ends, to the uterus and **vulF**. Rings are color-coded as in Fig. 1.

of a functional vulva. Previous work has characterized the molecular genetic basis of the fates of the six VPC cells (Greenwald, 1997; Kornfeld, 1997; Sternberg and Horvitz, 1989). Here we establish the cellular basis of vulval morphogenesis that provides a necessary developmental foundation for molecular genetic analyses of organ and pattern formation. We have shown that each half of the vulva develops autonomously implicating that interactions between the anterior and the posterior halves are not necessary for the execution of short-range migrations, toroid formation and intratoroidal fusions.

Role of cell fusion in vulval morphogenesis

Cell fusion is a process involved in entry of viruses into cells, fertilization, conjugation, and formation of muscle, bone and placenta (reviewed in (Hernandez et al., 1996). In *C. elegans*, 30% of all somatic nuclei are part of syncytia formed by cell fusion. We have previously characterized embryonic and postembryonic fusions in the hypodermis (Podbilewicz and White, 1994). In the development of the vulva, we observe six distinct types of topological cell fusion events:

(1) Heterotypic fusions of the daughters of P3.p, P4.p and P8.p with the syncytial hypodermis **hyp7** (**F_S**) (Fig. 1). Experiments have

shown that these cells are capable of acquiring vulval fates but fuse with **hyp7** because they are beyond the range of the inductive influence of the anchor cell (Sternberg and Horvitz, 1986; Sulston and White, 1980).

(2) Fusions between two pairs of anterior-posterior cells before toroid formation (**F_L**: longitudinal fusions between **vulA** precursors Fig. 3).

(3) Homotypic transverse fusions (**F_T**) between two pairs of **vulC** precursors (Figs 3, 5).

(4) Homotypic intratoroidal longitudinal fusions (**F_{IL}**) within **vulA**, **vulC**, **vulD** and **vulF**.

(5) Homotypic intratoroidal transverse fusions (**F_{IT}**) within **vulE** and **vulF** (Fig. 7).

(6) Heterotypic fusion of the anchor cell with **utse** (**F_{AC}**) opening up a channel between the uterus and vulva (Figs 4, 7).

One of the functions of heterotypic cell fusion in *C. elegans* development seems to be to suppress the expression of specific differentiated states (Podbilewicz and White, 1994). This is likely to be the reason for the **F_S** fusions in (1). The **F_{AC}** fusion in (6) could also be of this type only, in this case, the anchor cell fate has been expressed and may be only suppressed when the function of that cell is no longer required. Interestingly, evolutionary studies have shown that, in the development of the vulva in the nematode *P. pacificus*, cell death appears to be used as an alternative strategy to cell fusion (Eizinger and Sommer, 1997).

We conclude that AC and the descendants of the VPCs participate in the formation of the vulva resulting in:

(1) Specification of eight cell classes derived from the VPCs: **vulA**, **vulB1**, **vulB2**, **vulC**, **vulD**, **vulE**, **vulF** and **hyp7**.

(2) Formation of 7 syncytia: **hyp7**, **vulA**, **vulC**, **vulD**, **vulE**, **vulF** and **utse**.

The strategies used in the construction of the vulva in *C. elegans* are probably used in pattern formation during development of other organs. Very little is known about the mechanisms of migrations and fusions during the formation of

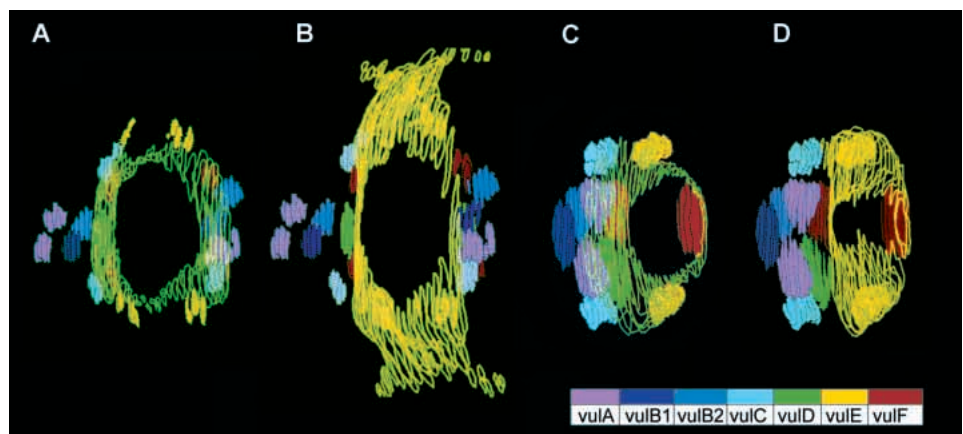


Fig. 9. Computer-generated graphic representation of ventral views of late L4 stage vulva and early L4 semi-vulva from serial section EM data. A, Vulva in a stage similar to Fig. 8 showing **VulD** ring (green outlines) and nuclei (shaded) from other toroids. (B) Same vulva as in A showing **vulE** ring (yellow outlines) that has sent projections attaching to the seam lateral epithelial cells at two points on either side. (C,D) Vulva where the posterior nuclei are absent (cells were killed by laser ablation); these are digitized details of the semivulva shown in Fig. 4F) and the anterior half has developed autonomously forming a stack of 7 toroidal rings, two of which are shown (C, **vulD**; D, **vulE**). Color code followed as in Fig. 1. Figures are oriented with the anterior of the worm on the left, and are ventral views.

different tissues in biological systems (Hernandez et al., 1996; Podbilewicz and White, 1994). Our results provide ideas for the analysis of organ formation and a way of correlating the lineage with the execution of cell migrations and cell fusions. Many pathological conditions in a variety of tissues contain syncytial cells most probably formed by cell fusion (Cross et al., 1994; Huang et al., 1993; Sitar et al., 1994). Gross vulval morphological defects have been identified in many mutants in *C. elegans*. The defective phenotypes have been described as reduced invagination at the mid-L4 stage, abnormal eversion of the vulva, 'squashed' vulva or development of abnormal vulval protrusion (Bettinger et al., 1997; Greenwald, 1997; Herman and Horvitz, 1997; Maloof and Kenyon, 1998; Seydoux et al., 1993). The exact nature of these defects in terms of cell-cell recognitions, interactions, fusions, migrations and attachments is not known. The detailed knowledge of short-range migrations, changes in cell shapes, cell fusions and the anatomical organization of the vulva allows a more precise description of the phenotypes of mutations that disrupt pattern formation in the vulva (unpublished observations).

We thank Bob Goldstein, David Gershon, Bill Mohler, Iva Greenwald, and members of the B. P. laboratory for valuable discussion and critical reading of the manuscript. Doug Kershaw undertook preparation and sectioning of samples for EM at the MRC Laboratory of Molecular Biology, Cambridge. Special thanks to Leanne Olds (Laboratory of Molecular Biology, Madison) for help in preparing illustrations and Vitaly Gofman for help in confocal microscopy. This research was supported by the Israel Science Foundation founded by the Israel Academy of Sciences and Humanities, the United States-Israel Binational Science Foundation (BSF), Jerusalem, the Israel Cancer Research Fund (ICRF), New York, and the Human Frontier Science Program Organization.

REFERENCES

- Baird, S. E., Fitch, D. A., Kassem, I. A. A. and Emmons, S. W. (1991). Pattern formation in the nematode epidermis: determination of the arrangement of peripheral sense organs in the *C. elegans* male tail. *Development* **113**, 515-526.
- Banerjee, U. and Zipursky, S. L. (1990). The role of cell-cell interactions in the development of the *Drosophila* visual system. *Neuron* **4**, 177-187.
- Bettinger, J. C., Euling, S. and Rougvie, A. E. (1997). The terminal differentiation factor LIN-29 is required for proper vulval morphogenesis and egg laying in *Caenorhabditis elegans*. *Development* **124**, 4333-4342.
- Brenner, S. (1974). The genetics of *Caenorhabditis elegans*. *Genetics* **77**, 71-94.
- Cross, J. C., Werb, Z. and Fisher, S. J. (1994). Implantation and the placenta: key pieces of the development puzzle. *Science* **266**, 1508-1518.
- Eizinger, A. and Sommer, R. J. (1997). The homeotic gene *lin-39* and the evolution of nematode epidermal cell fates. *Science* **278**, 452-454.
- Finney, M. and Ruvkun, G. (1990). The *unc-86* gene product couples cell lineage and cell identity in *C. elegans*. *Cell* **63**, 895-905.
- Francis, G. R. and Waterston, R. H. (1991). Muscle cell attachment in *Caenorhabditis elegans*. *J. Cell Biol.* **114**, 465-479.
- Freeman, M. (1997). Cell determination strategies in the *Drosophila* eye. *Development* **124**, 261-370.
- Grawe, F., Wodarz, A., Lee, B., Knust, E. and Skaer, H. (1996). The *Drosophila* genes crumbs and stardust are involved in the biogenesis of adherens junctions. *Development* **122**, 951-959.
- Greenwald, I. (1997). Development of the Vulva. In *C. elegans II*. (ed. D. Riddle, T. Blumenthal, B. Meyer and J. Priess), Vol. 33, pp. 519-541. Cold Spring Harbor, New York: Cold Spring Harbor Laboratory Press.
- Greenwald, I. and Rubin, G. M. (1992). Making a difference: the role of cell-cell interactions in establishing separate identities for equivalent cells. *Cell* **68**, 271-281.
- Greenwald, I. S., Sternberg, P. W. and Horvitz, H. R. (1983). The *lin-12* locus specifies cell fates in *Caenorhabditis elegans*. *Cell* **34**, 434-444.
- Hardin, J. (1989). Local shifts in position and polarized motility drive cell rearrangement during sea urchin gastrulation. *Dev. Biol.* **136**, 430-445.
- Herman, R. K. and Hedgecock, E. M. (1990). Limitations of the size of the vulval primordium of *Caenorhabditis elegans* by *lin-15* expression in surrounding hypodermis. *Nature* **348**, 169-171.
- Herman, T. and Horvitz, H. R. (1997). Mutations that perturb vulval invagination in *C. elegans*. *Cold Spring Harb. Symp. Quant. Biol.* **62**, 353-359.
- Hernandez, L. D., Hoffman, L. R., Wolfsberg, T. G. and White, J. M. (1996). Virus-cell and cell-cell fusion. *Annu. Rev. Cell Dev. Biol.* **12**, 627-661.
- Horvitz, H. R. and Sternberg, P. W. (1991). Multiple intercellular signalling systems control the development of the *Caenorhabditis elegans* vulva. *Nature* **351**, 535-541.
- Huang, T. W., Green, A. D., Beattie, C. W. and Das Gupta, T. K. (1993). Monocyte-macrophage lineage of giant cell tumor of bone. *Cancer* **71**, 1751-1760.
- Kimble, J. (1981). Alterations in cell lineage following laser ablation of cells in the somatic gonad of *Caenorhabditis elegans*. *Dev. Biol.* **87**, 286-300.
- Kornfeld, K. (1997). Vulval development in *Caenorhabditis elegans*. *Trends Genet.* **13**, 55-61.
- Maloof, J. N. and Kenyon, C. (1998). The Hox gene *lin-39* is required during *C. elegans* vulval induction to select the outcome of Ras signaling. *Development* **125**, 181-190.
- Newman, A. P., White, J. G. and Sternberg, P. W. (1996). Morphogenesis of the *C. elegans* hermaphrodite uterus. *Development* **122**, 3617-3626.
- Podbilewicz, B. (1996). ADM-1, a protein with metalloprotease- and disintegrin-like domains, is expressed in syncytial organs, sperm and sheath cells of sensory organs in *C. elegans*. *Mol. Biol. Cell* **7**, 1877-1893.
- Podbilewicz, B. and White, J. G. (1994). Cell fusions in the developing epithelia of *C. elegans*. *Dev. Biol.* **161**, 408-424.
- Reddi, A. H. (1994). Bone and cartilage differentiation. *Curr. Opin. Genet. Dev.* **4**, 737-744.
- Saxen, L. and Sariola, H. (1987). Early organogenesis of the kidney. *Pediatr. Nephrol.* **1**, 385-392.
- Seydoux, G., Savage, C. and Greenwald, I. (1993). Isolation and characterization of mutations causing abnormal eversion of the vulva in *Caenorhabditis elegans*. *Dev. Biol.* **157**, 423-436.
- Sitar, G., Bianchi, A. S., Rosti, V., Shaskin, P., Blago, R., Santamaria, L. and Ascari, E. (1994). Giant cell formation in Hodgkin's disease. *Res. Immunol.* **145**, 499-515.
- Sommer, R. J. (1997). Evolutionary changes of developmental mechanisms in the absence of cell lineage alterations during vulva formation in the Diplogastridae (Nematoda). *Development* **124**, 243-251.
- Sternberg, P. W. and Horvitz, H. R. (1986). Pattern formation during vulval development in *C. elegans*. *Cell* **14**, 761-772.
- Sternberg, P. W. and Horvitz, H. R. (1989). The combined action of two intercellular signaling pathways specifies three cell fates during vulval induction in *C. elegans*. *Cell* **58**, 679-693.
- Sulston, J. and Hodgkin, J. (1988). Methods. In *The Nematode Caenorhabditis elegans* (ed. W. B. Wood), pp. 587-606. Cold Spring Harbor, New York: Cold Spring Harbor Laboratory Press.
- Sulston, J. E. and Horvitz, H. R. (1977). Postembryonic cell lineages of the nematode *Caenorhabditis elegans*. *Dev. Biol.* **56**, 110-156.
- Sulston, J. E. and White, J. G. (1980). Regulation and cell autonomy during postembryonic development of *Caenorhabditis elegans*. *Dev. Biol.* **78**, 577-597.
- Thesleff, I. and Nieminen, P. (1996). Tooth morphogenesis and cell differentiation. *Curr. Opin. Cell Biol.* **8**, 844-850.
- Trinkaus, J. P. (1984). *Cells into organs - the forces that shape the embryo*. Englewood Cliffs, NJ: Prentice-Hall Inc.
- Wang, B. B., M.M., M.-I., Austin, J., Robinson, N. T., Chisholm, A. and Kenyon, C. (1993). A homeotic gene cluster patterns the anteroposterior body axis of *C. elegans*. *Cell* **74**, 29-42.
- White, J. G., Southgate, E., Thomson, J. N. and Brenner, S. (1986). The structure of the nervous system of *Caenorhabditis elegans*. *Philos. Trans. R. Soc. Lond. B Biol. Sci.* **314**, 1-340.
- Yap, A. S., Brieher, W. M. and Gumbiner, B. M. (1997). Molecular and functional analysis of cadherin-based adherens junctions. *Annu Rev Cell Dev Biol.* **13**, 119-146.